GEOLOGIA • 2009 • Tom 35 • Zeszyt 2/1 • 549–557

RECENT IMPROVEMENTS IN INTERPRETATION METHODOLOGY APPLIED IN GEOWIN SATUN APPLICATION

Aktualne udoskonalenia metodyki interpretacyjnej stosowanej w aplikacji Satun systemu GeoWin

Tomasz ZORSKI

Akademia Górniczo-Hutnicza, Wydział Geologii, Geofizyki i Ochrony Środowiska,
Katedra Geofizyki;
al. Mickiewicza 30, 30-059 Kraków;
e-mail: zorski@agh.geol.agh.edu.pl

Treść: Przedstawiono ostatnio wprowadzone udoskonalenia do aplikacji SATUN systemu interpretacji geofizyki wiertniczej GeoWin. Aplikacja SATUN jest interpretacyjnym narzędziem do analizy cienkowarstwowych utworów piaszczysto-ilastych pod kątem określania nasycenia węglowodorami. Kilkuletnie doświadczenia w stosowaniu aplikacji SATUN w warunkach gazonośnych formacji mioceńskich polskiego przedgórza Karpat skłoniły do wprowadzenia ulepszeń w metodyce. Po pierwsze, stały się dostępne nowe badania laboratoryjne rdzeni obejmujące analizy chemiczne i mineralogiczne, co pozwoliło wprowadzić nowe zależności z regresji wielokrotnej. Badania te potwierdziły wcześniej sygnalizowaną regułę, że przekrój czynny absorpcji neutronów Σ_a^{ma} jest w tym regionie ważnym wskaźnikiem zailenia. Bor okazał się głównym pierwiastkiem decydującym o rozkładzie Σ_a^{ma}. Po drugie, wprowadzono gęstościowo-neutronowy wykres krzyżowy jako alternatywny sposób określania porowatości i zailenia. Pokazano kompletny przykład polowy zastosowania zmodyfikowanej metodyki w sugerowanej nowej formie graficznej prezentacji wyników.

Słowa kluczowe: formacje cienkowarstwowe, zailenie w geofizyce wiertniczej, dekonwolucja w geofizyce wiertniczej, geofizyka wiertnicza

Key words: thin bedded formations, clay content and log data, deconvolution of log data, well logging

INTRODUCTION

Methodology background of well log interpretation in thin bedded gas bearing formations in the Carpathian Foredeep was described formerly (Zorski 2004). Application of this idea in GeoWin Well Log Interpretation System is presented in published manual of system (Jarzyna *et al.* 2007), in chapter "Aplikacja Satun". Methodology is permanently improved and some of new their aspects are presented in this paper.

The basic aim of Satun Application is reduction of strong resistivity masking effect caused by low resistive shale thin interbeds. Three levels of depth resolution are considered. The best resolution is obtained from six arm resistivity dipmeter, where beds as so thin as

1 centimetre can be detected. The middle level of the resolution is being reached by nuclear tools, for whom resolution is initially included between 10 and 50 centimetres. Their vertical resolution is improved by using deconvolution to raw measured data. The worse resolution is showed by deep range resistivity tool. This last resolution depends on accessible quality of resistivity tool. Raw dual induction (DIL) data give the resolution of about 1.2 m. It can be improved up to 0.6 m if sophisticated deconvolution is employed. The high resolution array induction tool (HRAI) delivers, on the other hand, the output curves which are processed by deconvolution procedures being fed into the computer system of tool. The highest vertical resolution reached by the HRAI tool is about 40 centimetres.

All these data must be put together and matched together for water saturation (S_w) calculation in thin permeable layers – the computer program SATUN was just made for this aim. Two sequences of layer borders are created. The first one includes the boundaries of thin layers distinguishable by the dipmeter, while the second one gives the boundaries for thick layers distinguishable by the deep range resistivity tool. Iterative calculations of rock resistivity (Zorski 2004) are performed inside of thick layers, which are divided on sequences of thin layers of sandstones and shales. These sequences are considered as a parallel sets of resistors, where sandstone water saturation S_w is changed in an optimising loop up to find the best agreement between calculated and measured resistivity of the thick layers. S_w of shale layers is arbitrarily assumed as equal to one. Resistivity of sand and shale layers is calculated using Waxman-Smits formula, where a few rock parameters must be known.

There are two types of improvements entered recently into interpretative procedures of the SATUN program. The first one concerns of new results of statistical analyses of rock samples data. As result, the better formulae are employed for calculation such parameters as CEC, clay content, bound water etc (Zorski *et al.* 2008). The second one is based on better using of accessible measuring equipment. Multidimensional output data of HRAI induction tool enabled better presentation of gas saturation results. The epithermal neutron porosity has been introduced, on the other hand, as independent indicator in determination both the porosity and the shale content.

BETTER DETERMINATION OF ROCK MATRIX PARAMETERS, BY USING THE REGRESSION FORMULAE

As was reported earlier (Zorski 2004), there exist two main sources of errors in gas saturation evaluation in thin bedded shaly-sand formations of Miocene Carpathian Foredeep. Masking effect of high electric resistivity as a result of the low vertical resolution of induction logs is a first and dominating source of these errors. Solution of this problem was main reason of the creation of SATUN software. Improper knowledge of the electric model of rock, however, is a second, also important, reason of errors. The proper electric model of rock enables the exact calculations of rock resistivity in dependence on both the shale parameters and the pore parameters.

A few years of experience in use of SATUN application and simultaneous research laboratory analyses confirm the Σ_a^{ma} as very useful logging signal (Zorski *et al.* 2008). The basic regression equations applied in calculation of CEC (Cation Exchange Capacity), SumClay (weight percent of sum illite-smectite, kaolinite and chlorite) and H2O (bound water) for interpretation of Now4 borehole are presented in table 1.

Table (Tabela) 1

Multivariate regression coefficients used in SATUN application of GeoWin interpretation system for Now4 borehole

Współczynniki regresji wielokrotnej użyte w aplikacji SATUN systemu GeoWin w interpretacji otworu Now4

Calculated variable *Obliczana zmienna*	Regression coefficients *Współczynniki regresji*				Determination coefficient R^2 *Współczynnik determinacji* R^2
	a_0	a_1	a_2	a_3	
CEC (mval/100g)	–11.9033	SigMa (cu)	GRAPI (API)	—	0.9637
		0.7394	0.0847	—	
Sum Clay (wt %)	–16.0826	SigMa (cu)	GRAPI (API)	—	0.9557
		1.2936	0.1536	—	
H2OP (vol %)	–3.4582	SigMa (cu)	—	—	0.9196
		0.4545	—	—	
H2OP (vol %)	0.8856	SigMa (cu)	Ca (wt %)	Fe (wt %)	0.9446
		0.2214	–0.4698	1.8436	
Ca (wt %)	9.9685	Pe (b/e)	Ca (wt %)	Fe (wt %)	0.9612
		–5.4463	2.1994	1.6252	
Si (wt %)	–33.4	Si (wt %)	SigMa (cu)	Ca (wt %)	0.9797
		2.7716	–0.3209	+1.1198	

Chlorine, however, arrives as the third important participant in logging signal. The only significant source of Cl in the analysed formation is formation water and NaCl can remain in rock samples after drying. It must be emphasised here, that for the above presented multivariate regression calculations the Σ_a^{ma} values were corrected for Cl content. The specific feature of the analysed Miocene formation is the variability of water salinity, both geographically and as a function of depth.

The statistical analysis disclosed that the Σ_a^{ma} is most important rock matrix indicator in Miocene formation. Calculation of participation of individual elements in Σ_a^{ma} were performed for three of analysed fields (ChD, Dzi, Now). Weighted averages of these participations and their standard deviations for most significant elements are presented in Table 2. It is well known (Herron & Matteson 1993) that some trace elements have dominant impact on the total neutron absorption cross section of rock. The microscopic cross sections of the discussed elements are listed in column 2 of Table 2. It simply means that such trace elements as B and Gd can be real competitors of main elements constituting the rock in Σ_a^{ma} participation. We can see that Boron participation in total Σ_a^{ma} for analysed Miocene rocks is near to 35%, while the average content of Boron is only 80 ppm. On the contrary, 65% of Si content generates no more than 14% of total Σ_a^{ma}. On the other hand, the impact of the element on total logging signal Σ_a^{ma} will depend not only on its average participation in Σ_a^{ma}, but on its variation in the whole formation, too. We can introduce then the some measure of Logging Signal "Power", calculated as a product of average participation of element in Σ_a^{ma} in formation and standard deviation of its participation (column 6 in table 2). The dominating Boron position can be clearly visible. Boron content in formation is a result of its adsorption to illite–smectite minerals and as consequence is the direct indicator of both the illite–smectite minerals content and CEC.

Water salinity ranges from 20 to more than 80 g/l and usually is it difficult to precisely predict it before final formation fluid testing. As a consequence, Cl is the source of interpretation noise. Introduction of the direct Si, Ca and Fe determination from log data using neutron spectral gamma tool seems to be the best way to reduce this effect. Al is best and direct clay indicator. Al emulator substitutes Al by linear combination of Si, Ca, Fe (Herron & Herron 1996). This idea was verified in many formations, and is working in analysed Miocene formation too – multivariate regression [Al (Si, Ca,Fe)] determination coefficient reaches value $R^2 = 0.988$ (Zorski *et al.* 2008). The introduction to interpretation procedures of both the Al emulator and Σ_a^{ma} could improve not only CEC and clay content calculation, but can also deliver information about NaCl presence.

Table (Tabela) 2

Results of calculations performed for explanation of influence of individual elements constituting the Miocene shaly-sand formation in the Carpathian Foredeep, on Σ_a^{ma}

Wyniki obliczeń przeprowadzonych w celu wyjaśnienia wpływu poszczególnych pierwiastków tworzących skały mioceńskie przedgórza Karpat na Σ_a^{ma}

Element *Pierwiastek*	Element microscopic neutron absorption cross –section (b) *Mikroskopowy przekrój czynny pierwiastka (b)*	Average Σ_a^{ma} participation [%] *Średni udział w Σ_a^{ma} [%]*	Standard deviation of Σ_a^{ma} participation [%] *Odchylenie stand. udziału w Σ_a^{ma} [%]*	Average content of element in rocks [%] *Średnia koncentracja pierwiastka w skale [%]*	Logging signal "power" *„Siła" sygnału profilowania*
1	2	3	4	5	6
B	767.000	34.866	7.339	0.00797	255.881
SiO_2	0.171	13.732	5.675	65.73007	77.930
Cl	33.500	10.941	4.637	0.16408	50.728
Fe_2O_3	5.121	6.826	1.694	3.41573	11.565
H_2O	0.665	5.526	1.665	2.47099	9.200
Gd	48890.000	7.885	1.012	0.00039	7.977
CaO	0.430	3.088	1.393	5.75544	4.302
K_2O	4.200	6.031	0.489	2.06830	2.948
Li	70.500	2.123	0.620	0.00342	1.316
Al_2O_3	0.463	2.738	0.331	9.46696	0.905
TiO_2	6.090	2.623	0.292	0.52655	0.765
Na_2O	1.060	1.590	0.371	1.33763	0.590

BETTER USING OF THE POSSIBILITY OF THE MEASUREMENT EQUIPMENT

The optimum, technically available set of logging tools in Miocene Carpathian Foredeep consists of tools as follows: dipmeter, density, high resolution array induction tool (HRAI) and thermal-epithermal neutron (NNTE). Dipmeter, commonly used for structural and the sedi-

mentological purposes, is applied here as thin layers indicator and as a source of shallow range resistivity. It substitutes the multi-electrode electrical micro imager being the modern option of dipmeter tool, which is not easy accessible in Poland unfortunately. Density logs improved in vertical resolution by deconvolution procedures are basic tool for porosity determination. HRAI is source of resistivity distribution around borehole for six spatial ranges, which change since 0.25 up to 3.0 m (10÷120 inches). The NNTE neutron tool delivers both the neutron porosity determined by means of the epithermal neutron flux analysis and neutron absorption cross section Σ_a^{ma}. New form of graphical presentation of data is suggested, enabling more comprehensive evaluation of both measurement and interpretation results.

The example of this new form is presented in figure 1, where results of calculation using of Satun GeoWin for Now4 borehole are visible, in comparison to traditional approach to logging data interpretation. Thirteen panels of graphical composition prepared in ProGeo software are set together in this figure. On the left of depth panel both raw data and results of preliminary interpretation of data are finding (Panels No. 1–4). On the right of depth panel the results of final interpretation are presented (Panels No. 6–13).

In panel 1: "Cal, Gr, SigMa", caliper and two lithology sensitive logs GR – total natural radioactivity and SigMa-neutron absorption cross-section Σ_a^{ma} are presented. Higher depth resolution of SigMa is noticed in comparison to GR resolution.

In panel 2: "Density, Neutron", two densities and neutron porosity determined from near epithermal detector of NNTE tool are considered. Special processing of Compensated Density Tool data delivers both, near space and far space (as result of Spine & Ribs corrections) densities. Near space density concerns the narrow cylindrical layer around borehole, not thicker than a few centimetres. Far space density concerns the rock located beyond this narrow near layer. These two densities are put together in the same scale and differences between them are shaded. Yellow shading corresponds to case when near density is bigger than far density. The green shading corresponds to inverse case. Comparing these two density curves to "Lith-Por SATUN" panel (6), the strong correlation between yellow shadings and sandstones can be disclosed. Increasing of near space density in permeable rocks can suggest that pore space is filled with the solid phase of drilling mud.

In panel 3: "Dipmeter" raw data from six dipmeter pads are presented. Values of curves are proportional to a resistivity of rock in very near vicinity of borehole wall. Spatial range of dipmeter electrodes does not exceed a few centimetres. It must be emphasised that these electrodes are not calibrated in resistivity units. The special procedure of resistivity calibration must be performed before dipmeter can be used as resistivity indicator of near space zone (Zorski 2004). Such calibrated resistivity curve is named as Rx0u_averPDD in panel. This curve corresponds to average value of all dipmeter arms. Because of deviation of borehole Now4 in angle about 30 degree, the dipmeter curves are shifted each to other. It simply means, the average of all pads is not good indicator of thin beds. In panel 5 two separate curves (Rx0_1 and Rx04) after resistivity calibration are exhibited for comparison to Rx0u_averPDD curve. These curves correspond to two opposite dipmeter arms numbered as 1 and 4.

In panel 4: "HRAI resistivity", the six ranges of resistivity in radial direction are put together. Presented curves HO01–HO12 correspond to six radially and vertically deconvolved resistivities. It simply means that vertical resolution of all these curves is about 40 cm and each curve corresponds to resistivity of different radial zone around borehole. Full range of these zones changes from 0.25 to 3.0 m.

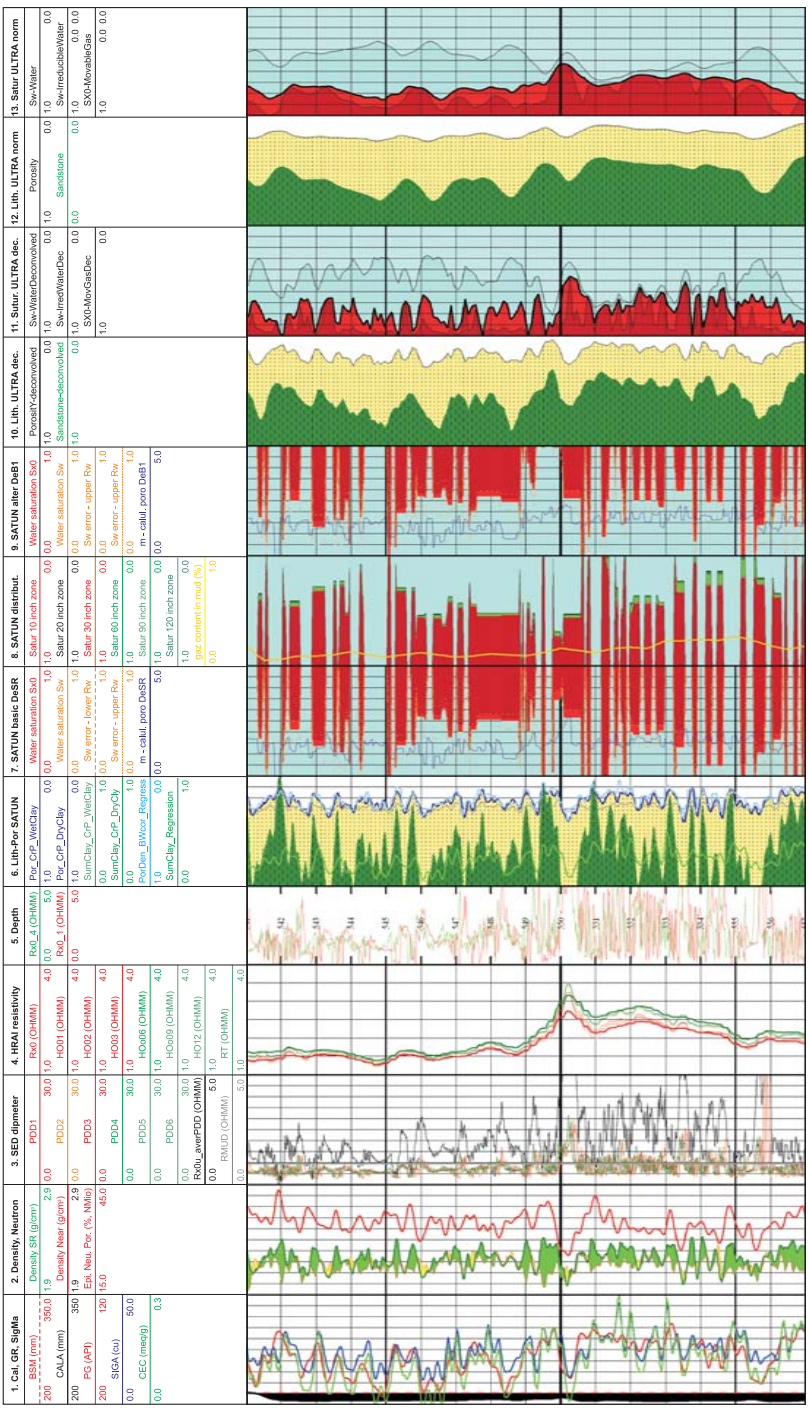

Fig. 1. Example of modified methodology applied to interpretation of depth interval 541÷557 m of Now4 borehole. Detailed discussion in text

Fig. 1. Przykład zastosowania zmodyfikowanej metodyki do interpretacji pomiarów w otworze Now4, interwał głębokościowy 541÷557 m. Szczegółowa dyskusja w tekście

In Panel 6: "Lith-Por SATUN", lithology and porosity are analysed. Two independent ways of litho-porosity calculation are available in current SATUN procedures. The first one, introduced recently and discussed in details later, is the litho-density crossplot. As result of crossplot application we get two different solutions, each of them for different Clay Point. Two Clay Points are introduced, the first one for Wet Clay and second one for Dry Clay. Finally, two Sum Clay curves and two Porosity curves are obtained – names visible in head of panel explain them directly. The second way of litho-porosity calculation use the regression formulae determining the Sum Clay and bound water (H2OP) listed in Table 1. The porosity obtained in this option is firstly calculated from bulk density, assuming average matrix density determined in laboratory by means of helium pycnometer, and secondly corrected by subtraction of bound water.

In Panels 7, 8 and 9 the water saturation calculations, using SATUN software, are presented. Panels 7 and 9 are almost identical in graphical form. The different input porosities, however, were assumed as starting points in calculations both the *m* coefficient. Basic calculations presented in panel 6 were performed using bulk rock density, corrected by "Spine & Ribs" procedure – this kind of density corresponds to far space. Alternative calculation (Panel 9) was performed using near space density delivered by near detector of density tool. In both cases the saturation calculations were performed using Rx0 and RT resistivities delivered by HRAI tool procedures. Lower and upper envelopes of *Sw* errors are presented too. These errors correspond to +/– 30% fluctuations of formation water resistivity *Rw* around the value assumed in *Sw* calculation. In Panel 8 the distribution of water saturation in radial zones around the hole is presented. The radially deconvolved resistivities HO01-HO12, delivered by HRAI tool procedures were used in these calculations. Yellow continuos curve presents the analysis of gas content in mud, measured directly during drilling, by drilling lab service.

In Panels 11–13 results both the litho-prosity and the saturation analysis made by means of ULTRA software are presented. Two different set of input data were applied. First is exploiting deconvolved density curves (Panels 10, 11), while the other is exploiting standard density curves (Panels 12, 13).

DENSITY-NEUTRON CROSS-PLOT AS ALTERNATIVE WAY OF LITHO-POROSITY ANALYSIS

The crucial problem in cross-plot technique application in shaly-sand formation is proper determination of clay point (La Vigne *et al.* 1994). The two clay points need to be considered if smectite or illite–smectite minerals are abundant in rock. Measurements and calculations performed for four fields widespread in Carpathian Foredeep allow precisely define these points (Środoń, Kawiak 2009). Analyses of mineral and chemical compositions shows that the Miocene formation is homogeneous. It allows apply the correlation relations defined in one field to the another fields. The comprehensive analyses of chemical and mineralogical data, using special BESTMIN software, were performed for Dzików field (Środoń *et al.* 2006). These results were transformed into Nowosielec field, where the coordinates of clay points were determined (Tab. 3). Constructed cross-plot diagram is presented in figure 2. It concerns the chosen depth interval (541÷557 m) of Now4 borehole. In figure the red points correspond to core data, while blue points correspond to log data.

Table (Tabela) 3

Clay points coordinates defined using the chemical and mineralogical analyses for density-neutron cross-plot working in Miocene formation of Carpathian Foredeep

Współrzędne punktów iłu dla gęstościowo-neutronowego wykresu krzyżowego stosowanego w mioceńskich utworach przedgórza Karpat, określone na podatawie chemicznych i mineralogicznych analiz rdzeni

	Density dry clay point [g/cm^3] *Gęstość dla punktu suchego iłu [g/cm^3]*	Density wet clay point [g/cm^3] *Gęstość dla punktu mokrego iłu [g/cm^3]*	NeuEpiBli dry clay point [%] *Punkt NeuEpiBli dla suchego iłu [%]*	NeuEpiBli wet clay point [%] *Punkt NeuEpiBli dla mokrego iłu [%]*
Number *Liczebność*	65.00	65.00	65.00	65.00
Average *Średnia*	2.86	2.57	16.59	31.55
Stand. Dev. *Odch. Stand.*	0.04	0.07	1.88	3.10
Max.	3.03	2.81	21.83	38.48
Min.	2.81	2.43	12.88	24.39

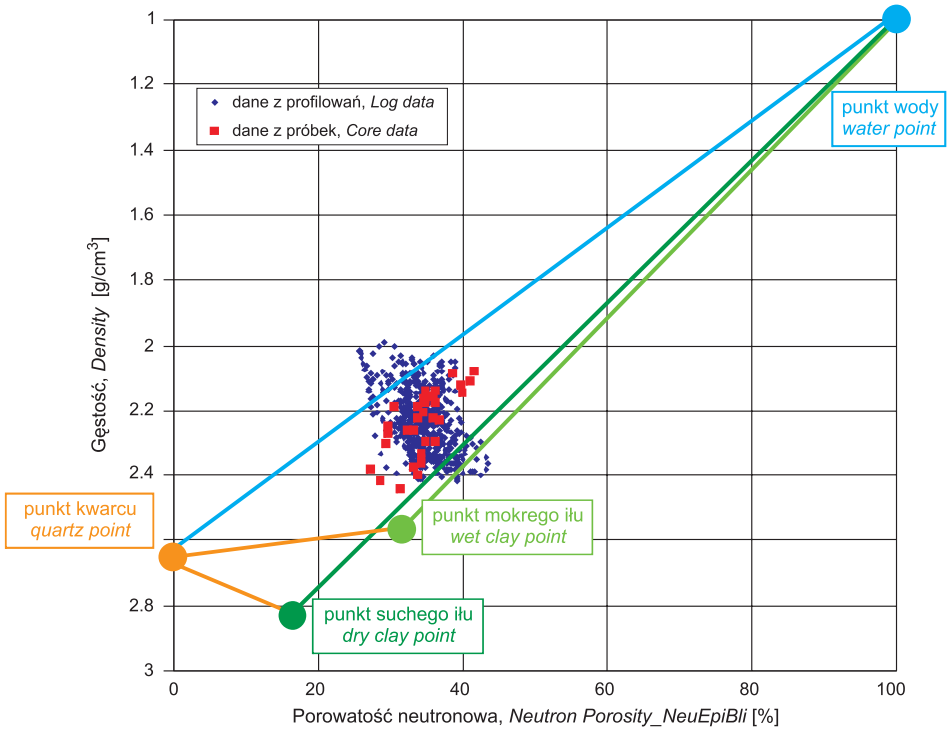

Fig. 2. Cross-Plot Density S&R vs NeuEpiBli, Now4

Fig. 2. Gęstościowo-neutronowy wykres krzyżowy (neutrony epitermiczne) Now4

It must be noticed that Clay Points presented in Table 3 exhibit some fluctuations, dependent on clay composition. Correlation between these parameters (density of clay and epithermal neutron porosity of clay) and logging lithology indicators like Σ_a^{ma}, Pe, GR, Si, Ca and Fe shows direction of future improvement of cross-plot procedure.

Presented results has been obtained during performance of the research project sponsored by Ministry of Science and Higher Education (Decision No. 620/E-77/SN-007/2006), Scientific Net: "Nuclear Methods for Geophysics"; Coordinated by Institute of Nuclear Physics PAS, Kraków.

Praca była prezentowana na VII Konferencji Naukowo-Technicznej pt. „Geofizyka w geologii, górnictwie i ochronie środowiska" organizowanej z okazji jubileuszu 90-lecia AGH na WGGiOŚ.

REFERENCES

Jarzyna J., Bała M., Cichy A., Gądek W., Karczewski J., Marzencki K., Stadtmüller M., Twaróg W. & Zorski T., 2007. *Przetwarzanie i interpretacja profilowań geofizyki wiertniczej system GeoWin cz. II. Nowe aplikacje i uzupełnienia* (Jarzyna J. Ed.). AGH, WGGiOŚ, Zakład Geofizyki, Geofizyka Kraków Sp. z o.o., Kraków, 1–86.

Herron M.M. & Matteson A., 1993. Elemental Composition and Nuclear Parameters of Some Common Sedimentary Minerals. *Nuclear Geophysics*, 7, 383–406.

Herron S.L. & Herron M.M., 1996. Quantitative Lithology: An Application for Open and Cased Hole Spectroscopy. *SPWLA 37th Annual Logging Symposium, June 16–19, 1996*, E.

Środoń J., Mystkowski K., McCarty D.K. & Drits V.A., 2006. BESTMIN: A computer program for refining the quantities and the chemical composition of clays and other mineral components of fine-grained rocks. *International Conference "Clays and Clay Minerals", Pushchino, Russia*, Abstracts, 41.

Środoń J. & Kawiak T., 2009. Chemical and mineralogical data and their interpretation based on BESTMIN analysis. Prepared to publication.

La Vigne J., Herron M. & Hertzog R., 1994. Density-Neutron Interpretation in Shaly Sands. *SPWLA 35th Annual Logging Symposium, June 19–22, 1996*, EEE.

Zorski T., 2004. Methodology of well log interpretation in thin-bedded gas bearing formations in Carpathian Foredeep (in Polish). *Geologia (kwartalnik AGH)*, 30, 275–298.

Zorski T., Ossowski A. & Środoń J., 2008. Mineral composition and petrophysical parameters evaluation from well logging data: Carpathian Foredeep example. *MECC'08, 4th Mid-European Clay Conference, September 22–27, 2008, Zakopane, Mineralogia*, Special Papers, 33, 192.